

MULTI-FREQUENCY TEMPERATURE MODULATION FOR METAL-OXIDE GAS SENSORS

R Gutierrez-Osuna^{1*}, S Korah¹ and A Perera²

¹Computer Science Dept., Wright State University, Dayton, OH 45435 (US)

²Dept. d'Electrònica, Universitat de Barcelona, 08028 Barcelona (Spain)

ABSTRACT

This article presents an empirical study of temperature modulation for metal-oxide gas sensors at multiple frequencies ranging from 0.125Hz to 4Hz. Commercial metal-oxide sensors from two manufacturers were exposed to analyte concentrations below their isothermal discrimination threshold over a period of ten days. The results reported in this article indicate that temperature modulation can significantly increase the selectivity of the sensors with respect to isothermal operation, yielding classification rates on test data close to 100%. The effects of heater voltage frequency and drift on the two sensors, as well as drift compensation procedures, are also discussed.

1 INTRODUCTION

The selectivity of metal-oxide semiconductor (MOS) gas sensors is greatly influenced by the operating temperature of the device, since the reaction rates for different volatile compounds and the stability of adsorbed oxygen species are a function of surface temperature [1, 2]. This temperature-selectivity dependence can be utilized to improve the selectivity of MOS sensors by cycling the operating temperature during exposure to volatile compounds and processing the dynamic response of the sensor.

A slow-changing heater voltage is desirable as it allows the sensor to reach the set-point temperature and, therefore, approach quasi-isothermal operation within a small time window. In this case, the temperature-modulated pattern from one sensor becomes equivalent to the response of multiple isothermal MOS sensors at different temperatures. Slow temperature cycles, however, increase the duration of sampling times. Thus, from a practical standpoint, it is interesting to determine the fastest temperature cycle that still preserves the dynamic characteristics of the sensor (e.g., sensitivity peaks).

This article addresses the effect of different temperature-modulation frequencies on the information content of the resulting sensor patterns. The stability of these patterns over time is also analysed, as sensor drift is a strong limiting factor in current gas sensor technology.

* To whom correspondence should be addressed (rgutier@cs.wright.edu). This research was supported by awards from WSU/OBR Research Challenge and Initiation, and NSF/CAREER 9984426.

2 EXPERIMENTAL SET-UP

Two commercial MOS sensors from different manufacturers were used in this study: TGS2610 and SB11A [3, 4]. Heater-voltage control was used as an approximation to operating-temperature or heater-resistance control [5]. In order to reduce cooling effects caused by effluent flow [6], the sensors were introduced in 30ml glass vials through a tight aperture on the cap, as shown in Figure 1(a), and allowed to equilibrate with the static headspace of 10ml of the analyte.

The instrumentation circuit shown in Figure 1(b) was used to control the heater voltage and acquire the temperature-modulated responses. The heater voltage set-point was generated with a LabVIEW-controlled multi-function data-acquisition card (National Instruments PCI 6024E) and subsequently current-boosted with a Darlington pair. The sensitive element was placed in a standard half-bridge configuration, and the voltage across a load resistor R_L (10k Ω for TGS2610 and 20k Ω for SB11A) was acquired into the computer.

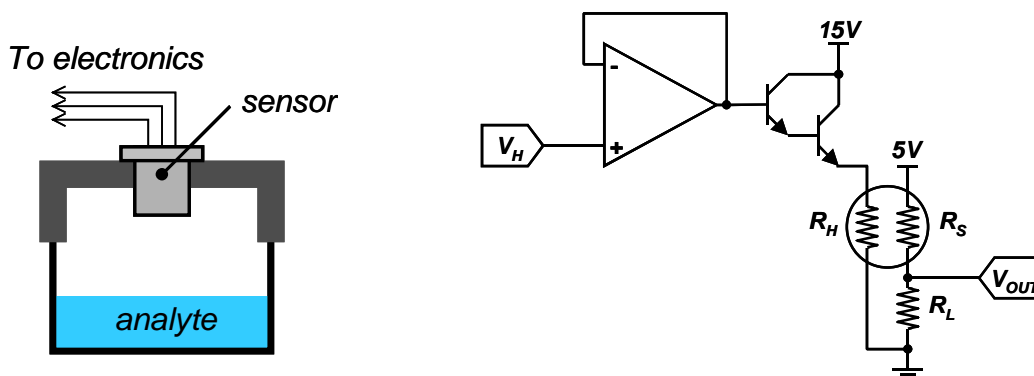


Figure 1. Static headspace setup (a) and instrumentation circuit (b)

Four household products were employed for this study: white vinegar (5% v/v acetic acid), ammonia, isopropyl alcohol and acetone. Due to their different vapor pressures, these analytes can be readily discriminated with conventional isothermal excitation. In order to determine if temperature modulation could increase the selectivity of the sensors, each analyte was serially diluted in water until the isothermal sensor response was similar for the four analytes. Therefore, the sensors were operated at concentration levels below the isothermal discrimination threshold. The final dilutions were 100% for vinegar, 28% for ammonia, 0.8% for isopropyl alcohol and 0.08% for acetone. Figure 2 shows the steady-state isothermal response of each sensor for the final dilutions (each dot represents an example). Room-air samples were also collected as a reference.

Upon insertion on the sample vial, the sensor heater was excited with a voltage profile that contained ten minutes of DC excitation at the nominal heater voltage recommended by the manufacturer (5V for TGS, 0.9V for FIS), followed by six sinusoidal segments (0-7V amplitude for TGS, 0-0.9V for FIS) at 0.125Hz, 0.25Hz, 0.5 Hz, 1 Hz, 2 Hz and 4Hz, ten cycles each. Sinusoidal waveforms were chosen due to their smoothness and continuity, which allows the sensor temperature to follow the heater voltage more closely. The response of the sensor was acquired with a sampling rate of 100Hz.

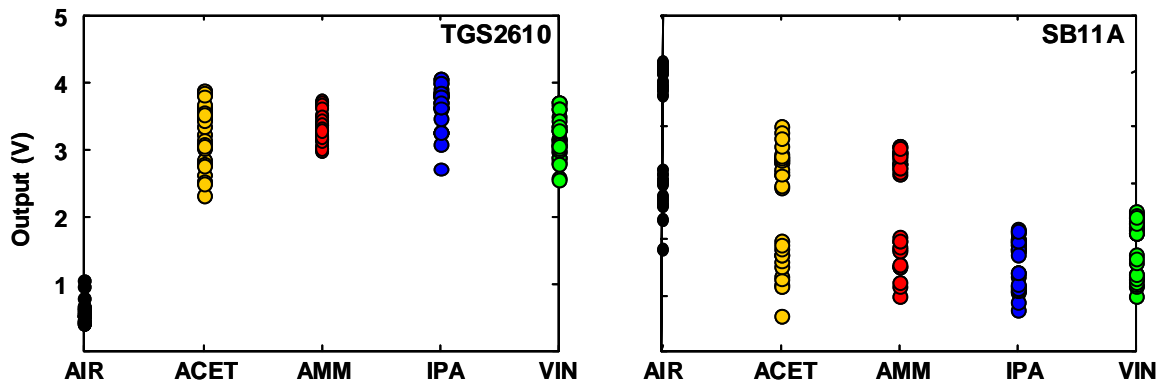


Figure 2. Isothermal steady-state response of the final serial dilutions

Figure 3 shows the heater profile for the TGS and the response of both sensors to reference room air. As shown in the figure, the amplitude of the sensor response decreases at higher frequencies since the sensors cannot cool down fast enough as a result of thermal inertia. The response of the sensors to the different analytes was collected for ten consecutive days to assess the stability of the temperature-modulated patterns. Each analyte was sampled three times per day, for a total of 150 examples per sensor. The presentation order of the fifteen daily samples was randomised to reduce sequential correlations.

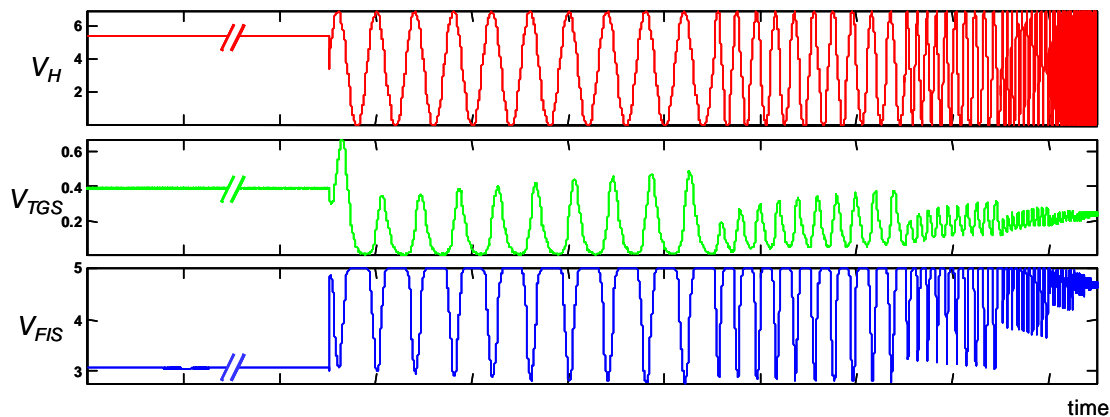


Figure 3. Heater voltage profile for TGS (top), and half-bridge response to room air for TGS (middle) and FIS (bottom)

3 RESULTS

The results of these experiments are summarized in **Figure 4**, which shows the average response of each sensor to the various analytes at 0.125Hz, 0.5Hz and 2Hz. For visualization reasons, the sensor response has been converted to conductance (Ω^{-1}) and only the ninth temperature cycle (out of ten) is shown. As predicted by the theory [7], the conductance of the sensors increases at higher heater voltages and also in the presence of the analytes.

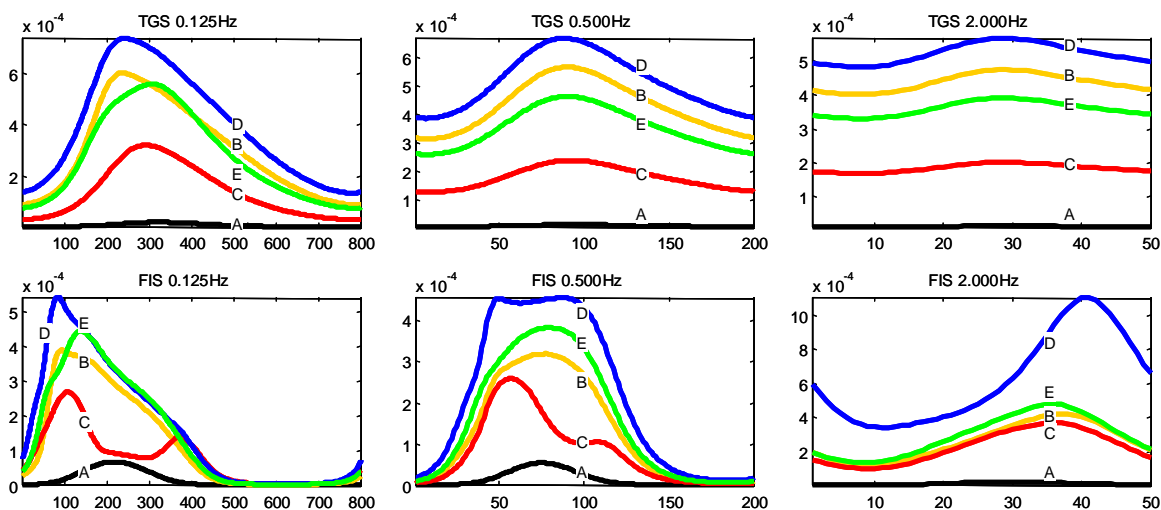


Figure 4. Average conductance of TGS and FIS at various heater frequencies to air (A), acetone (B), ammonia (C), IPA (D) and vinegar (E)

These results clearly show that the response of both sensors is more discriminative at lower frequencies, since the sensors approach a quasi-isothermal behavior at multiple temperatures. In the case of FIS, two peaks in conductance are resolved, which correspond to the optimum catalytic reaction temperature for the analyte gas [2]. As the frequency increases, each sensor response approaches the isothermal behavior at the root mean-squared value of the heater waveform and, therefore, the information content is no longer in the shape of the signal (dynamic) but rather in its DC offset (static).

In the remaining sections of this article, the discriminatory power and stability of the temperature-modulated responses are analysed using only a single temperature cycle, as shown in **Figure 4**. It is possible, however, that additional information could be extracted from the remaining temperature cycles and their exponential envelopes.

4 DISCRIMINATION PERFORMANCE

In this section the information content of the temperature-modulated responses is analysed. Rather than extracting shape-descriptors (e.g., position and value of the peaks) or fitting parametric models to the waveforms (e.g., see [8]), which may not capture enough discriminatory information, feature vectors for the analytes were obtained with a simple sub-sampling procedure. Although the lower frequencies could afford a higher-dimensional feature vector¹, all the frequencies were sub-sampled down to 25 samples to prevent differences in dimensionality from distorting the predictive accuracy estimates for each frequency. Linear Discriminant Analysis (LDA) was also used to further reduce the dimensionality of the feature vector down to four dimensions [9]. Classification was performed with the k Nearest Neighbors voting rule [10]. A value of k equal to one-half the number of examples per class was used throughout the experiments reported in this article.

Predictive accuracy was estimated using ten-fold cross-validation, where each fold was associated to all the examples from a particular day of data collection. The average results for both sensors at each frequency are summarized in Table 1. The classification rate for

¹ A fixed sampling rate of 100Hz was used regardless of cycling frequency.

isothermal data is also included as a baseline. In this case, the steady-state value of the sensor response after the 10-minute isothermal segment was used as a single, scalar feature. The results shown in Table 1 clearly indicate that temperature modulation can increase the performance of the two sensors beyond the isothermal discrimination threshold. As expected, better performance is obtained at lower temperatures, although FIS provides recognition rates close to 100% for frequencies up to 1Hz.

Table 1. Predictive accuracy versus frequency

Freq (Hz)	DC	0.125	0.25	0.5	1	2	4
Figaro	51	100	97	85	85	75	67
FIS	47	99	99	97	96	87	73

5 PATTERN STABILITY

The temperature-modulated responses are, unfortunately, subject to drift. Figure 5(a)-(b) shows the response of each sensor for a particular analyte throughout the experiment (30 examples, 10 days). It can be observed that drift is primarily multiplicative (an amplitude change) but also additive (a DC offset). Although both sensors are affected by drift, the TGS responses are more stable. Drift, rather than sensitivity, appears to be the limiting factor in these experiments.

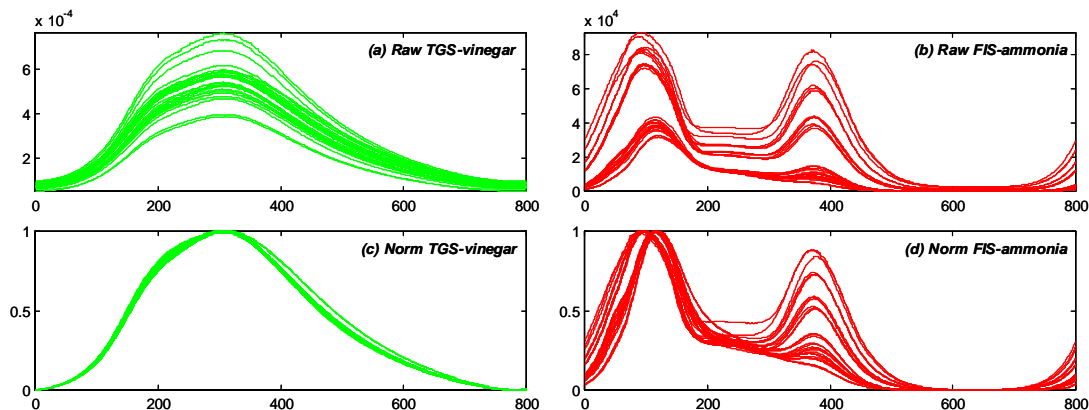


Figure 5. Drift effect for TGS-vinegar (left) and FIS-ammonia (right) patterns before (top) and after (bottom) baseline and amplitude normalization.

In order to quantify the stability of the temperature-modulated data over time, a sequential pattern analysis on the ten data-collection days is performed next. Shown in Figure 6, this analysis estimates the predictive accuracy of a particular classifier as a function of the training set size, denoted by N , and the time-stamp differences the training and test days, denoted by D . With increasing values of N , the training set incorporates data from more days, which allows the pattern classifier to automatically average out the drift component² [11]. With increasing values of D , on the other hand, the training dataset may become increasingly obsolete as a result of drift.

² This is presumably the mechanism that allowed FIS to outperform TGS in Table 1.

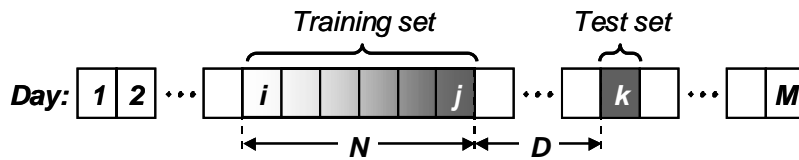


Figure 6. Training set size (N) and drift (D) in a sequential dataset

To emphasize the stability of the temperature-modulated patterns, a value of $N=1$ is chosen. This means that the LDA-KNN classifier is trained on data from a single day. The predictive accuracy as a function of D ($1 < D < 7$) for both sensors and the six cycling frequencies is shown Figure 7(a)-(b). These results are consistent with those shown in Figure 5(a)-(b), and indicate that the TGS provides temperature-modulated patterns that are more stable with time.

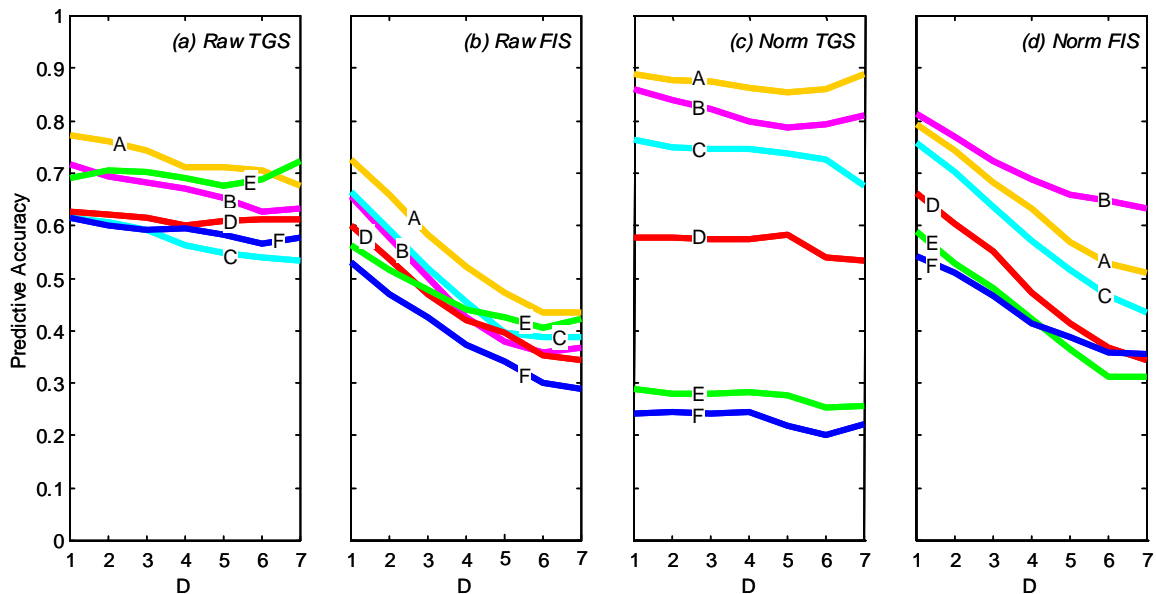


Figure 7. Predictive accuracy of the sensors as a function of drift at different frequencies (A=0.125Hz, F=4Hz)

5.1 DRIFT-COMPENSATION

To determine if preprocessing the patterns can help compensate for drift, each pattern was normalized by subtracting its minimum value and dividing by its peak-to-peak amplitude. As a result, the normalized signals do not contain DC or amplitude information, which implies that subsequent pattern-classification is performed solely on the basis of waveform shape. Figure 5(c)-(d) shows the response of the sensors after normalization. Although the repeatability of both sensors is improved after normalization, the TGS response proves to be more amenable to this type of pre-processing. The resulting predictive accuracy estimates as a function of drift are shown in Figure 7(c)-(d), which indicate that normalization can provide better drift-compensation at low frequencies, since these responses contain sufficient shape-related information. At higher frequencies, particularly for TGS, normalizing the patterns actually degrades the performance since the information is primarily in the DC offset of the signal.

6 DISCUSSION

The performance of temperature-modulation as a function of heater voltage frequency was studied on two commercial MOS sensors. Experimental results indicate that, for the particular set of analytes employed in this article, (1) temperature modulation improves the isothermal discrimination threshold for both sensors, (2) lower heater frequencies contain more discriminatory information, and (3) temperature-modulated patterns are affected by sensor drift.

Gain and offset normalization can be utilized to compensate for drift and stabilize the sensor patterns, particularly for TGS at low heater frequencies. It is also possible that the repeatability of the patterns may be improved at higher concentrations, since the experiments reported in this article were performed below the isothermal discrimination threshold. Finally, the stability of temperature-modulated patterns over longer time periods (e.g., weeks or months) needs to be studied and constitutes a clear direction for future research.

7 REFERENCES

- [1] Madou M J and Morrison S R 1989, *Chemical Sensing with Solid State Devices*, Academic Press, Boston MA.
- [2] Lee A P and Reedy B J 1999, *Sensors and Actuators B*, 60(1), pp. 35-42.
- [3] Figaro 1996, Figaro Engineering, Inc., Osaka, Japan.
- [4] FIS 1998, FIS Inc., Osaka, Japan.
- [5] K. Ihokura and J. Watson (1994), *The Stannic Oxide Gas Sensor*, CRC Pr., Boca Raton.
- [6] Mielle P 1996, *Sensors and Actuators B* 34, pp. 533-538.
- [7] Clifford P K and Tuma D T 1982, *Sensors and Actuators* 3, pp. 233-254.
- [8] Wlodek S and Colbow K 1991, *Sensors and Actuators B*, 3, pp. 63-68.
- [9] Duda R O, Hart P E and Stork D G 2001, *Pattern Classification*, Wiley, New York.
- [10] Fukunaga K 1990, *Statistical Pattern Recognition*, Academic Pr., San Diego, CA.
- [11] Gutierrez-Osuna R 2000, *Electronic noses and olfaction 2000* (Gardner J W and Persaud K C, Eds.), Bristol: Institute of Physics Publishing.